OPTOELECTRONICS AND ADVANCED MATERIALS – RAPID COMMUNICATIONS Vol. 3, No. 12, December 2009, p. 1290 - 1294

Structural and electrochemical characterization of Zn-TiO_2 nanocomposite coatings electrodeposited on steel

A. V. POP[*], A. VLASA[a], S. VARVARA[b], B. DAVID, C. BULEA[c], L. MURESAN[a]
Department of Physics, "Babes-Bolyai" University, 400028 Cluj-Napoca, Romania
[a]*Department of Physical Chemistry, "Babes-Bolyai" University, 400028 Cluj-Napoca, Romania*
[b]*Department of Topography, "1 Decembrie 1918" University Alba-Iulia, Romania*
[c]*BETAK S.A., Str. Industriilor, 4 Bistrița, Romania*

The structural, morphological, electrochemical and the corrosion behavior of Zn-TiO_2 nanocomposite coatings obtained by electrolytic co-deposition on steel substrate is presented. The influence of TiO_2 nanopaticles concentration on the increase of corrosion resistance of composite coatings is discussed. An improved corrosion resistance was obtained for a composite obtained for a concentration of 5g/l TiO_2 nanopaticles in the plating bath.

(Received November 06, 2009; accepted November 23, 2009)

Keywords: Zn-TiO_2 composite coatings, XRD, SEM, AFM, Electrolytic co-deposition, Corrosion

1. Introduction

The coating onto steel has long been established as an effective and reliable method for corrosion protection [1]. Zinc coated steel sheets are widely used as corrosion resistant materials, but the life span of such coatings is limited due to the aggressive nature of some environments, particularly those containing industrial pollutants. Consequently, considerable efforts are being made to improve their corrosion resistance [2].

Zinc composites containing occluded TiO_2 particles offer an interesting solution to this problem, due to their improved corrosion and wear resistance, increased hardness and better tribological properties as compared to pure zinc coatings [3].

One of the most attractive methods to obtain composite coatings with zinc matrices is electrolytic codeposition. The method combines the advantages of metal electroplating (such as low cost and versatility) with those of composite materials, resulting in advanced materials with tailor-made properties [4].

The electrolytic codeposition of zinc with TiO_2 particles by using micron or submicron size particles suspended in a classical zinc electroplating bath has been already reported [2, 5-7]. A lot of parameters, such as current profile, bath composition, pH, particle concentration, temperature, stirring rate, presence of additives, strongly influence the properties of the resulting composite coatings [8]. Due to the complexity of the process, there are still many unknown aspects to be considered.

The aim of this work is to investigate the influence of the nature and concentration of TiO_2 nanoparticles on the properties of Zn-TiO_2 composite films plated on steel substrate, by using non-electrochemical (X ray diffraction, atomic force microscopy) and electrochemical (open circuit potential and polarization curves) methods.

2. Experimental

2.1 Materials

Two types of TiO_2 nanoparticles, (Alfa Aesar, AA, 99,9%, 32 nm, Anatase) and Degussa, D, 99,5%, 21 nm) were suspended in an aqueous electrolyte containing 75 g/l $ZnCl_2$, 230 g/l KCl, 20 g/l H_3BO_3 and brightening agents. The concentration of TiO_2 nanoparticles in the plating bath was 3 g/l, 5g/l and 10 g/l, respectively.

For corrosion tests a solution of 0.2 g/l $(NH_4)_2SO_4$ (Riedel –de Haën, Germany) (pH 3) was used. All other reagents were analytical graded and were used as received.

2.2 Electrodes preparation

The electrodeposition of the Zn-TiO_2 nanocomposite films was carried out in a two compartments glass cell, using a disk electrode of OL 37 steel (S = 0.5024 cm^2) as working electrode, a $Ag/AgCl/KCl_{sat}$ as reference electrode and a Pt foil as a counter electrode. Before electrodeposition, the working electrode was wet polished on emery paper of different granulations and finally it was polished on felt with a suspension of alumina. The coatings were obtained at a constant current density ($i=10mA/cm^2$) by using a potentiostat/galvanostat (Voltalab PGP201, Radiometer analytical), during 30 minutes, at room temperature (25 +/- 2°C). The TiO_2 nanoparticles were maintained in suspension by using a magnetic stirrer (stirring rate 200 rpm).

2.3 Morphological and structural analysis

The microstructures and the distribution of chemical phases on the surface of the as-electrodeposited Zn-TiO_2 nanocomposite films were analyzed by atomic force microscope (AFM). The chemical composition of the Zn-

TiO_2 nanocomposite films was determined using an EDAX NEW XL30 X-ray dispersive energy analyzer attached to the scanning electron microscopy (SEM), using a Philips XL-30 microscope. The deposit structure and the preferred orientation of crystallites were determined by X-ray diffraction (XRD) analysis, using a Brucker X-ray diffractometer with a Cu K_α (λ = 0.15406 nm) at 45 kV and 40 mA. The 2θ range of 20–100º was recorded at the rate of 0.02ºand 2θ /0.5 s. The crystal phases were identified comparing the 2θ values and intensities of reflections on X-ray diffractograms with JCP data base using a Diffrac AT-Brucker program.

2.4 Electrochemical measurements

The corrosion measurements (open circuit potential and polarization curves) were performed with a potentiostat Autolab-PGSTAT 10, (Eco Chemie BV, Utrecht, Netherlands). Open-circuit potential (*ocp*) measurements were carried out as a function of time, during 1 hour. Anodic and cathodic polarization curves were recorded in a potential range of E = E_{corr} ± 200 mV for kinetic parameters determination and in a potential range of E = E_{corr} ± 20 mV for polarization resistance determination, with a scan rate of 0.25 mV s^{-1}.

3. Results and discussion

3.1 Structural and morphological analysis

The X-ray diffractograms of Zn-TiO_2 nanocomposite for different TiO_2 (Degussa) nanoparticles content in the plating bath are shown in Fig. 1. The diffraction peaks of zinc phase, and the substrate (iron) are present in all investigated nanocomposite.

By increasing TiO_2 concentration from 0g/l to 5g/l, the intensity of (101) peak of Zn decreases and the reflection (100) increases. The intensity for (101) peak increases in sample 11a (10g/l) and it becomes comparable with the intensity of (110) peak. The observed textural modifications of composite coatings are associated with specific structural modifications of Zn crystallites determined by adsorption - desorption phenomena occurring on the metal surface [9], induced by the presence of TiO_2 nanoparticles

The mean crystallite dimensions D were obtained from the (110) linewidth of XRD line [10-12]. The profile of (001) peak shows a Lorentz type behavior-Fig.2 The calculated value for D by using Scherrer equation [10], shows that an increase in TiO_2 concentration from zero to 10 g/l, leads to a decrease in grain size from 28.7 nm to 24 nm . For sample 10a (TiO_2 concentration 5g/l), the mean crystallite size is D=24.2 nm.

Localized EDAX analysis carried out on the coating cross-sections indicated that there is no significant difference in the chemical composition of studied samples (Table 1).

Table 1. Chemical composition of the samples.

Element	O	Cl	K	Ti	Fe	Zn
Weight%	3.78	0.35	0.08	0.00	2.76	93.02
Atomic%	13.75	0.57	0.13	0.00	2.88	82.68

The results in Table 1 show that along the cross section, there is no presence of Ti atoms. In order to emphasize if Ti or TiO_2 nanoparticles are distributed over the surfaces, Phase Imaging-AFM was recorded.

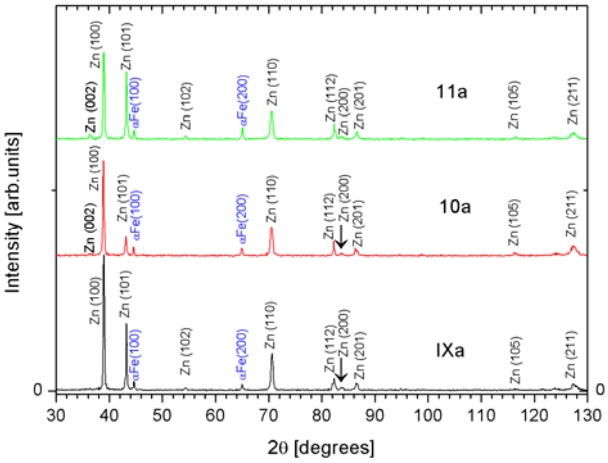

Fig. 1. XRD of Zn-TiO_2 nanocomposite for 0 g/l (sample IX), 5g/l (sample 10a) and 10 g/l (sample 11a) concentration of TiO_2 nanoparticles in the plating bath.

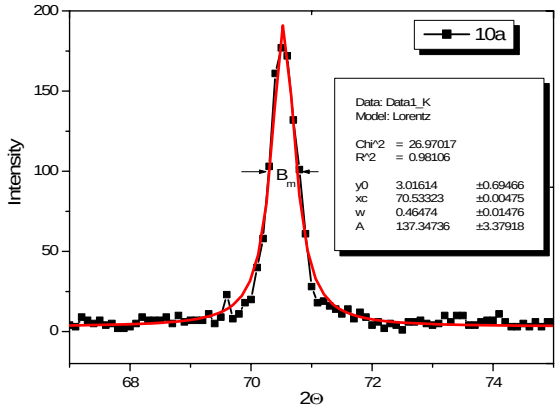

Fig. 2. The profile of (110) peak of Zn film 10a .The smooth curve shows the Lorentz fit of data.

By mapping the phase of the cantilever oscillation during the Tapping Mode scan, phase imaging goes beyond simple topographical mapping by detecting variations in composition, and perhaps other properties.

According to figure 3 there is a difference in phase distribution on the coating surfaces. The TiO_2 nanoparticles are evidenced by the small dark dots, uniform distributed on the surface of sample 10a, and the dark elongated islands on the surface of sample 11a.

The elongated islands suggest the clustering of TiO_2 nanoparticles. Supplementary, on the surface of 11a sample, the lighter islands suggest an additional phase. It is obvious that sample 10a has a better surface homogeneity than sample 11a.

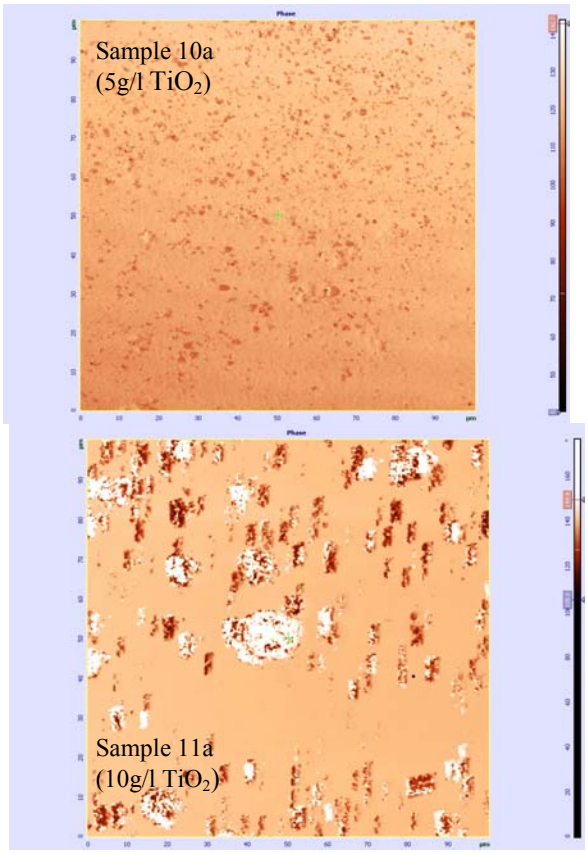

Fig. 3. AFM phase imaging for samples 10a (5g/l TiO_2) and 11a (10g/l TiO_2).

3.2 Open circuit potential(ocp) measurements

The open-circuit potentials values for Zn and Zn-TiO_2 coatings, recorded after 1 h of immersion in 0.2 g/l $(NH_4)_2SO_4$ solution (pH 3) are presented in Table 2.

Except for the case of the Zn-10 g/l TiO_2 (AA) coating, the *ocp* values of the composite layers are more positive than the one corresponding to the pure Zn deposit, which could be associated to an inhibition of the anodic reaction and consequently to a higher corrosion resistance.The more negative value of the *ocp* in the case of Zn-10 g/l TiO_2 (AA) deposit, suggests an acceleration of the corrosion process in the presence of 10 g/l TiO_2 (AA). This behavior is related to the defects and dislocations or to chemical heterogeneities generated in the metallic matrix by the embedded particles (see Fig. 3).

Table 2. Open circuit potential values for the corrosion of Zn and Zn-TiO_2 coatings.

TiO_2 (g/l)	Open circuit potentials (V *vs.* Ag/AgCl)	
	Degussa	Alfa Aesar
0	-1.019	-1.019
3	-1.015	-1.009
5	-1.011	-0.992
10	-1.005	-1.030

3.3 Polarization curves

The cathodic and anodic polarization curves of Zn and Zn-TiO_2 coatings recorded after 1h of immersion in $(NH_4)_2SO_4$ solution (pH 3) are presented in figure 4. From the polarization curves, the corrosion parameters were evaluated by using the relation:

$$i = i_{corr} \{\exp[b_a (E-E_{corr})] - \exp[b_c (E-E_{corr})]\} \quad (1)$$

where b_a and b_c are the anodic and cathodic activation coefficients, respectively.

The results obtained in the absence and in the presence of the two different types (DD and AA) of TiO_2 nanoparticles in the deposit are presented in Table 4.

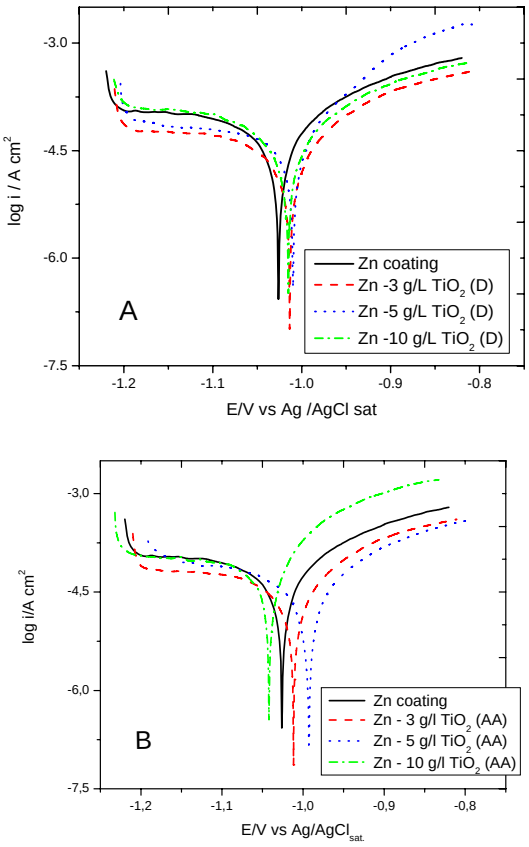

Fig. 4. Polarization curves for Zn, Zn-TiO_2 Degussa (D) and Zn-TiO_2 Alfa Aesar (AA) coatings in 0.2 g/L $(NH_4)_2SO_4$ (pH =3); scan rate 0.25 mV s^{-1}.

Table 4. The corrosion parameters calculated from the polarisation curves.

TiO_2	TiO_2 conc. in the bath (g/l)	E_{cor} (V)	i_{cor} ($\mu A/cm^2$)	b_a (V^{-1})	- b_c (V^{-1})	R'_p (Ω cm^2)
-	0	-1.027	110	11.44	4.14	583.5
Alfa Aesar	3	-1.016	70	16.38	9.26	557.2
	5	-0.999	60	11.19	8.01	866.6
	10	-1.051	140	14.95	6.84	327.9
Degussa	3	-1.019	50	18.76	9.98	695.9
	5	-1.016	40	24.41	7.37	785.2
	10	-1.018	90	10.95	4.76	707.3

The polarization resistivities R_p were determined from the slope of polarization curves ($\Delta E/\Delta i$) recorded in a potential range of $E = E_{corr} \pm 20$ mV.

Polarization resistivity $R_p = R'_p$ may be obtained from the Stern-Geary equation :

$$R_p^{-1} = 2.303 i_{corr}\left(\frac{1}{B_a} + \frac{1}{B_c}\right) \quad (2)$$

In equation (2), the polarization resistance relates to the corrosion behavior of the metal which freely and uniformly corrodes in a homogenous medium. The physical (defects and dislocations) and chemical heterogeneity (the presence of Zn oxides, TiO_2 particles or impurities) of Zn coatings disturbs the electrochemical electrode reactions (which may proceed faster in some places, while being inhibited in other places). Therefore, the resistance calculated from equation (2) is denoted by symbol R'_p since it is an approximate value, in comparison with R_p determined close to $E_{corr} \pm 20$ mV, [13].

As can be seen from Table 4, the values of the corrosion parameters in the presence of TiO_2 change in comparison with pure Zn coating, which indicates that the TiO_2 particles influence the kinetics of both the anodic and cathodic processes. The difference between the values of the kinetic parameters corresponding to the two types of coatings could be explained by the different fraction, grain size and crystalline structure of the embedded TiO_2 particles.

Except for the case of Zn-10 g/l TiO_2 (AA) coating, the corrosion current density decreases in all cases in the presence of embedded TiO_2 as compared with the value corresponding to the pure Zn coating. This suggest that the incorporation of TiO_2 particles in the metallic deposit has a beneficial effect on its corrosion resistance. The highest corrosion resistance was observed in the case of the composite coatings obtained from electrolytes containing 5 g/l TiO_2. Thus, the corrosion resistance is determined by two opposite effects. On one side, the embedded inert oxide particles diminish the active surface in contact with the corrosive environment [15], and on the other side they disturb the crystallization process, by generating dislocations and defects in the metallic matrix which act as chemical heterogeneities and favor the corrosion process [16].

The non-uniform distribution of TiO_2 nanoparticles in the coating obtained for 10g/l nanoparticles (fig.3), arises because particles easily agglomerate in aqueous plating electrolytes, [17]. As a consequence, the codeposition of agglomerated particles takes place and the anticipated mechanical, chemical and/or physical properties of the composite coatings are not achieved. Recently, the improved protection provided by the coatings containing TiO_2 nanoparticles on aluminium alloy was obtained [18,19]. This result is attributed to the TiO_2 particle-rich thin film layer formed on the outer part of the coating.

4. Conclusions

The XRD shows only diffraction pattern characteristic from Zn film as well as the substrate (steel).

The increase of TiO_2 concentration in electrolyte solution up to 5g/l, leads to the textural modifications, evidenced by change in the peaks intensities (100) and (101), and to the decrease of mean grain size. The coating obtained with 5g/l TiO_2 shows the better chemical homogeneity of surface (AFM phase imaging) and the best anticorrosion properties.

TiO_2 Degussa confers better corrosion protection to the zinc coatings than TiO_2 Alfa Aesar nanoparticles.

By increasing the nanoparticles concentration above the optimal concentration (5 g/l TiO_2), the corrosion protection decreases because of the non-uniform distribution and the clustering of TiO_2 nanoparticles.

Acknowledgments

The authors gratefully acknowledge the financial support from project NANOTECH 97/28.09.2007

References

[1] Z. Abdel Hamid, Anti-Corrosion Methods and Materials **48**(4), 235 (2001).

[2] A. Gomes, M. I. Da Silva Pereira, M. H. Mendonça, F. M. Costa, J. Solid State Electrochem. **9**, 190 (2005).
[3] T. T. Tuaweri, G. D. Wilcox, Surface Coat. Technol. **200**, 5921 (2006).
[4] A. Hovestad, L. J. J. Jansen, J. Appl. Electrochem. **25**, 519 (1995).
[5] P. B. Mokshanatha, V. T. Venkatarangaiah, N. Y. Arthoba, P. Kalappa, Synthesis and Reactivity in Inorganic, Metal-Organic and Nano-Metal Chemistry **37**(6), 461 (2007).
[6] L. Muresan, M. Gherman, I. Zamblau, S. Varvara, C. Bulea, Studia Universitatis Babes-Bolyai, Chemia **LII**(3), 97 (2007).
[7] T. Deguchi, K. Imai, H. Matsui, M. Iwasaki, H. Tada, S. Ito, J. Mat. Sci**. 36**, 4723 (2001).
[8] C. T. J. Low, R. G. A. Wills, F. C. Walsh, Surface Coat. Technol. **201**, 371 (2006).
[9] J. Amblard, M. Froment, N. Spyrellis, Surf. Technol. **5**, 205 (1977).
[10] H. P. Klug, L. E. Alexander, X-ray Diffraction Procedures, 2nd edition (John Wiley, New York, 1974).
[11] D. Balzar, J. Appl. Cryst. **25,** 559 (1992).
[12] Th. Kehagias, Ph. Komninou, G. Nouet, P. Ruterana, Th. Karakostas*, Phys. Rev. B* **64**, 195329 (2001).
[13] B. Szczygieł, M. Kołodziej, Electrochim. Acta **50**, 4188 (2005)
[14] F. Fontenay, L. B. Andersen, P. Moller, Galvanotechnik **92**, 928 (2001).
[15] A. Gomes, M. I. Da Silva Pereira, M. H. Mendonça, F. M. Costa, J. Solid State Electrochem. **9**, 190 (2005).
[16] A. Hovestad, L. J. J. Jansen, J. Appl. Electrochem. **25**, 519 (1995)
[17] J. P. Fransaer, E. Leunis, T. Hirato, J. P. Celis, J. Appl. Electrochem. **32**, 123 (2002).
[18] O. Zubillaga, F. J. Cano, I . Azkarate, I. S. Molchan, G. E. Thompson, A. M. Cabral, P. J. Morais, Surface & Coatings Technology **202**(24), 2008.
[19] O. Zubillaga, F. J. Cano, I . Azkarate, I. S. Molchan, G. E. Thompson, P. Skeldon, Surface & Coatings Technology **203**(10-11), 2009.

*Corresponding author: avpop@phys.ubbcluj.ro